Influence of Thermal Radiation on Free Convection adjacent to a Sphere in Porous Media: Considering Soret and Dufour Effects

Kuo-Ann Yih

Department of Aircraft Engineering, Air Force Institute of Technology

Abstract

Influence of thermal radiation on free convection adjacent to a sphere in porous media considering Soret and Dufour effects is numerically analyzed. The surface of the sphere is maintained at uniform wall temperature and concentration. The governing equations are transformed into dimensionless, non-similar forms by using suitable non-dimensional variables and then solved by Keller box method. Numerical data of the dimensionless temperature and concentration profiles, the Nusselt and Sherwood numbers are presented by graphic and tabular forms in the four parameters: the dimensionless coordinate ξ , the Soret parameter S, the Dufour parameter D, and the radiation parameter R.

Keywords: Soret and Dufour effects, free convection, sphere, porous media, thermal radiation

多孔性介質內熱輻射對於流經球體自然對流的影響:考慮索瑞特/杜福效應

易國安 空軍航空技術學院飛機工程系

摘要

本文以一數值方法來分析在多孔性介質內熱輻射對於流經球體自然對流的影響:考慮索瑞特/杜福效應。球體的表面為均勻壁溫度與濃度。吾人先以適宜的無因次變數,將原始的控制方程式轉換成一組無因次非相似的型式,再以凱勒盒子法來解之。本文數值計算的結果藉由圖形與表格的形式來顯示,四個參數:無因次座標、索瑞特參數、杜福參數、熱輻射參數,對於無因次溫度與濃度分佈、紐塞爾和希爾吾德數之影響。

關鍵字:索瑞特與杜福效應,自然對流,球體,多孔性介質,熱輻射

1. Introduction

The study of combined heat and mass transfer by natural convection in a porous medium has many engineering application problems such as geothermal systems and petroleum engineering applications. A comprehensive account of the available information in this field is provided in recent books by Bejan [1] and Nield and Bejan [2].

In the field of the saturated porous medium, Yamamoto [3] studied the free convection about a sphere in using series method (SM). The problem of natural convection boundary layers on isothermal

axi-symmetric (e.g., sphere) of arbitrary shape was presented by Merkin [4] using the similarity solution (SS). Cheng [5] extended the research of Merkin [4] to study the mixed convection about a sphere for the case of uniform wall temperature (UWT). Minkowycz et al. [6] extended the work of Cheng [5] to analyze numerically the mixed convection about a nonisothermal sphere with variable wall temperature (VWT) by using the local non-similarity method (LNSM). Huang et al. [7] used Keller box method (KBM) to investigate the mixed convection flow over a sphere for the uniform heat flux case. Nakayama and Koyama [8] studied the free convective heat transfer over a nonisothermal body of arbitrary shape by local non-similarity method and integral method (IM). Forced convection flow past a sphere at large Peclect numbers was examined by Pop and Yan [9] by using the analytical solution (AS). Yih [10] used the KBM to investigate viscous and Joule heating effects on non-Darcy MHD natural convection flow over a permeable sphere with internal heat generation. Cheng [11] analyzed free convection heat transfer from a sphere using a thermal non-equilibrium model by the cubic spline collocation method (CSCM). In the aspect of coupled heat and mass transfer, Lai and Kulacki [12] studied coupled heat and mass transfer from a sphere buried by series solution. Chamkha et al. [13] presented the non-similar solution for convective boundary layer flow over a sphere saturated with a nanofluid.

The Dufour (diffusion-thermal) and Soret (thermo-diffusion) effects have important role on the geosciences and chemical engineering. Huang [14] utilized the KBM to examine the influence of non-Darcy and MHD on free convection of non-Newtonian fluids over a vertical permeable

plate with Soret/Dufour effects and thermal radiation. Moorthy et al. [15] discussed the Soret and Dufour effects on natural convection heat and mass transfer flow past a horizontal surface with variable viscosity. Soret/Dufour effects on coupled heat and mass transfer by free convection over a vertical permeable cone with internal heat generation and thermal radiation was reported by Huang [16]. Cheng [17] analyzed the Soret and Dufour effects on free convection boundary layer over a vertical cylinder. Yih [18] investigated free convection about a permeable horizontal cylinder with Soret/Dufour effects for uniform heat flux and uniform mass flux (UHF/UMF). However, concerning the study of the case of sphere is lacking.

The aim of the present work, therefore, is to investigate the effects of Dufour/Soret on natural convection flow past a sphere in porous media.

2. Analysis

Consider the problem of the Soret and Dufour effects on combined heat and mass transfer by free convection flow past a sphere with uniform wall temperature and uniform wall concentration embedded in a porous medium. Figure 1 shows the flow model and physical coordinate system.

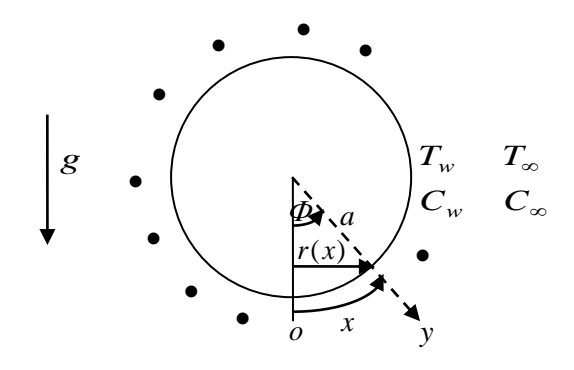


FIG. 1 The flow model and physical coordinate system

The wall temperature T_w and wall concentration C_w are higher than the ambient temperature T_∞ and ambient concentration C_∞ . x is measured along the circumference of the sphere from the lowest point o and y is measured normal to the surface. a is the radius of the sphere. $\Phi = x/a$ is the angle of the y-axis with respect to vertical $(0 \le \Phi \le \pi)$. $r(x) = a \sin(x/a) = a \sin \Phi$ is the local radius of the sphere. The gravitational acceleration g is acting downward.

The flow over the sphere is assumed to be two-dimensional, laminar and steady. We also assumed that the boundary layer thickness is sufficiently thin compared with the radius of the sphere.

Introducing the laminar boundary layer approximation $(\partial/\partial x << \partial/\partial y, \ v << u, \ \delta << a)$, Boussinesq approximation (all the fluid properties are assumed to be constant, except for density variation in the buoyancy term), and Rosseland diffusion approximations, the governing equations and the boundary conditions based on the Darcy law (valid for low velocity) can be written as follows:

Conservation of mass:

$$\frac{\partial(ru)}{\partial x} + \frac{\partial(rv)}{\partial y} = 0,\tag{1}$$

Conservation of momentum (Darcy law):

$$u = \frac{g \sin \Phi K}{V} \left[\beta_T \left(T - T_{\infty} \right) + \beta_C \left(C - C_{\infty} \right) \right], \quad (2)$$

Conservation of energy:

$$u\frac{\partial T}{\partial x} + v\frac{\partial T}{\partial y} = \alpha \frac{\partial^2 T}{\partial y^2} - \frac{1}{\rho C_P} \frac{\partial q_r}{\partial y} + \overline{D} \frac{\partial^2 C}{\partial y^2},$$

Conservation of concentration:

$$u\frac{\partial C}{\partial x} + v\frac{\partial C}{\partial y} = D_M \frac{\partial^2 C}{\partial y^2} + \overline{S}\frac{\partial^2 T}{\partial y^2}, \tag{4}$$

Boundary conditions:

$$y = 0: v = 0, T = T_w, C = C_w,$$
 (5)

$$y \to \infty$$
: $T = T_{\infty}$, $C = C_{\infty}$. (6)

where, u and v are the velocities in the x- and y- directions, respectively; K is the permeability of the porous medium; v is the kinematic viscosity; β_T and β_C are the thermal and concentration expansion coefficients of the fluid, respectively; T and C are the volume-averaged temperature and concentration, respectively; q_r is the radiation heat flux; α and D_M are the equivalent thermal diffusivity and mass diffusivity, respectively; \overline{D} and \overline{S} are the Dufour coefficient and Soret coefficient of the porous medium, respectively.

The stream function ψ is defined by

$$ru = \partial(r\psi)/\partial y$$
 and $rv = -\partial(r\psi)/\partial x$, (7)

therefore, the continuity equation is automatically satisfied.

Using the Rosseland diffusion approximation , the radiation heat flux is given by

$$q_r = -\frac{4\sigma}{3k^*} \frac{\partial T^4}{\partial y} \tag{8}$$

where σ is the Stephan–Boltzmann constant and k^* is the absorption coefficient. Huang [16] obtained that the temperature differences within the flow are assumed to be sufficiently small so that T^4 may be expressed as a linear function of temperature T using a Taylor series expansion about the ambient temperature T_∞ ; and neglecting the higher order terms, we can obtain the following relationship:

$$T^{4} = T_{\infty}^{4} + 4T_{\infty}^{3} (T - T_{\infty}) = 4T_{\infty}^{3} T - 3T_{\infty}^{4}$$
 (9)

Combining equations (8)-(9), thus the radiation heat flux can be simplified as follows:

$$q_r = -\frac{16\sigma T_\infty^3}{3k^*} \frac{\partial T}{\partial y} \tag{10}$$

Invoking the following dimensionless variables:

(3)

$$\xi = \frac{x}{a} \tag{11}$$

$$\eta = \frac{y}{a} R a^{\frac{1}{2}} \tag{12}$$

$$f(\xi,\eta) = \frac{\psi}{\alpha \ \xi \ Ra^{\frac{1}{2}}} \tag{13}$$

$$\theta(\xi,\eta) = \frac{T - T_{\infty}}{T_{w} - T_{\infty}} \tag{14}$$

$$\phi(\xi,\eta) = \frac{C - C_{\infty}}{C_{w} - C_{\infty}} \tag{15}$$

$$Ra = \frac{g\beta_T (T_w - T_\infty) Ka}{v\alpha}$$
 (16)

where ξ is the dimensionless coordinate, η is the pseudo-similarity variable, f is the dimensionless stream function, θ is the dimensionless temperature, ϕ is the dimensionless concentration, Ra is the modified Rayleigh number for the flow through the porous medium.

Inserting equations (10)-(16) into equations (2)-(6), (10), we get the following results:

Dimensionless governing equations:

$$f' = \frac{\sin \xi}{\xi} (\theta + N\phi), \tag{17}$$

$$\left(1 + \frac{4}{3}R\right)\theta'' + \left(1 + \frac{\xi \cos \xi}{\sin \xi}\right)f\theta' + D\phi''$$

$$= \xi \left(f'\frac{\partial \theta}{\partial \xi} - \theta'\frac{\partial f}{\partial \xi}\right),$$
(18)

$$\frac{1}{Le}\phi'' + \left(1 + \frac{\xi \cos \xi}{\sin \xi}\right) f\phi' + S\theta''$$

$$= \xi \left(f' \frac{\partial \phi}{\partial \xi} - \phi' \frac{\partial f}{\partial \xi}\right).$$
(19)

Dimensionless boundary conditions:

$$\eta = 0: f = 0, \theta = 1, \phi = 1,$$
(20)

$$\eta \to \infty$$
: $\theta = 0$, $\phi = 0$. (21)

In the above, the primes denote differentiation with respect to η .

In addition, the other important parameters are also defined as following:

$$N = \frac{\beta_C \left(C_w - C_\infty \right)}{\beta_T \left(T_w - T_\infty \right)} \tag{22}$$

$$Le = \frac{\alpha}{D_M} \tag{23}$$

$$R = \frac{4\sigma T_{\infty}^3}{k^* k} \tag{24}$$

$$D = \frac{\overline{D}(C_w - C_\infty)}{\alpha(T_w - T_\infty)}$$
 (25)

$$S = \frac{\overline{S}(T_w - T_\infty)}{\alpha(C_w - C_\infty)}$$
 (26)

where N, Le, R, D, and S denote the buoyancy ratio, the Lewis number, the radiation parameter, the Dufour parameter, and the Soret parameter, respectively.

The results of practical interest in many applications are both heat and mass transfer rates. They are expressed in terms of the Nusselt number *Nu* and the Sherwood number *Sh* respectively, which are defined as follows:

$$Nu = \frac{ha}{k} = \frac{q_w a}{(T_w - T_\infty)k} = \frac{\left[-k\left(\frac{\partial T}{\partial y}\right)_{y=0} + q_r\right]a}{(T_w - T_\infty)k}$$

$$= \frac{-\left(1 + \frac{16\sigma T_\infty^3}{3kk^*}\right)\left(\frac{\partial T}{\partial y}\right)\Big|_{y=0}}{T_w - T_w} a$$
(27)

$$Sh = \frac{h_m a}{D_M} = \frac{m_w a}{(C_w - C_\infty)D_M} = \frac{-\left(\frac{\partial C}{\partial y}\right)\Big|_{y=0}}{C_w - C_\infty}. \quad (28)$$

with the help of equations (11)-(16), the Nusselt number Nu and the Sherwood number Sh in terms of $Ra^{\frac{1}{2}}$ are, respectively, obtained by

$$\frac{Nu}{Ra^{\frac{1}{2}}} = \left(1 + \frac{4}{3}R\right) \left[-\theta'(\xi,0)\right] \tag{29}$$

$$\frac{Sh}{Ra^{\frac{1}{2}}} = -\phi'(\xi,0). \tag{30}$$

3. Results and Discussion

The solution for the system of equations (17)-(21) is by using the Keller box method described in the work of Huang and Yih [19] with $\Delta \xi = 0.01$, the first step size $\Delta \eta_1 = 0.01$, and $\eta_\infty = 50$. The variable grid parameter is chosen as 1.01.

In order to verify the accuracy of our present method, we have compared our results with those of Bejan [1] and Merkin [4]. Table 1 shows the comparison of $[-\theta'(\xi,0)]$ for various values of ξ with N=D=R=S=0. The comparison in the above case is found to be in good agreement.

Table 1 Comparison of $[-\theta'(\xi,0)]$ for various values of ξ with N=D=R=S=0

ξ	$\left[- heta'(\xi,\!0) ight]$			
	Bejan [1]	Merkin [4]	Present results	
0.0	0.8880	0.8875	0.8875	
0.2	0.8821	0.8816	0.8816	
0.4	0.8644	0.8639	0.8639	
0.6	0.8351	0.8347	0.8346	
0.8	0.7946	0.7941	0.7941	
1.0	0.7432	0.7428	0.7428	
1.2	0.6817	0.6813	0.6813	
1.4	0.6108	0.6104	0.6104	
1.6	0.5318	0.5315	0.5315	
1.8	0.4464	0.4461	0.4461	
2.0	0.3568	0.3566	0.3566	
2.2	0.2664	0.2662	0.2662	
2.4	0.1797	0.1796	0.1796	
2.6	0.1029	0.1029	0.1029	
2.8	0.0432	0.0432	0.0432	
3.0	0.0077	0.0077	0.0076	
$\pi =$	0.0000	0.0000	0.0000	
3.14	0.0000	0.0000	0.0000	

Since the effects of the buoyancy ratio N and the Lewis number Le have been discussed by Lai and Kulacki [12]. Therefore, in this paper, the

numerical results are mainly presented for the Dufour parameter D ranging from 0 to 0.3, the Soret parameter S ranging from 0 to 0.3, the dimensionless coordinate ξ ranging from 0 to π = 3.14, the radiation parameter R ranging from 0 to 5, with N=3, and Le=2.

The dimensionless temperature concentration distributions for two values of the radiation parameter R (R = 0, 5) and the dimensionless coordinate ξ (ξ = 0.0, 2.0) with N = 3, Le = 2, D = 0.1, S = 0.1 are shown in Figs. 2 and 3, respectively. At the given R = 5, increasing the dimensionless coordinate ξ from 0.0 (red line) to 2.0 (blue line) has the tendency to increase the thermal boundary layer thickness as well as the concentration boundary layer thickness. For the given $\xi = 0.0$, increasing the radiation parameter R from 0 (black dashed line) to 5 (red line) reduces the dimensionless surface temperature gradient $|-\theta'(\xi,0)|$ but increases the dimensionless surface concentration gradient $[-\phi'(\xi,0)]$, displayed in Figs. 2 and 3.

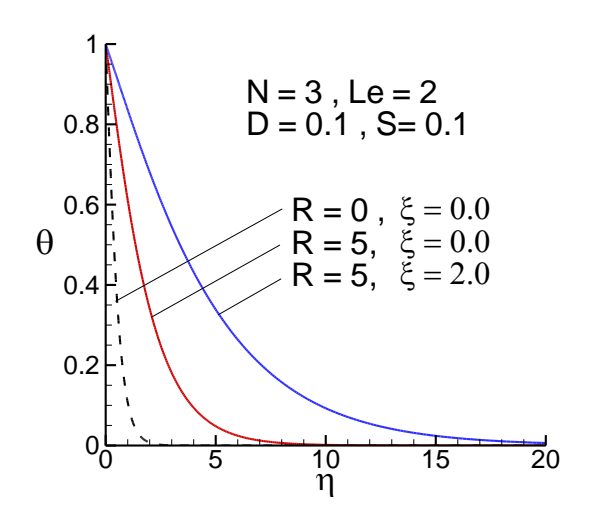


FIG. 2 The dimensionless temperature distributions for two values of ξ and R

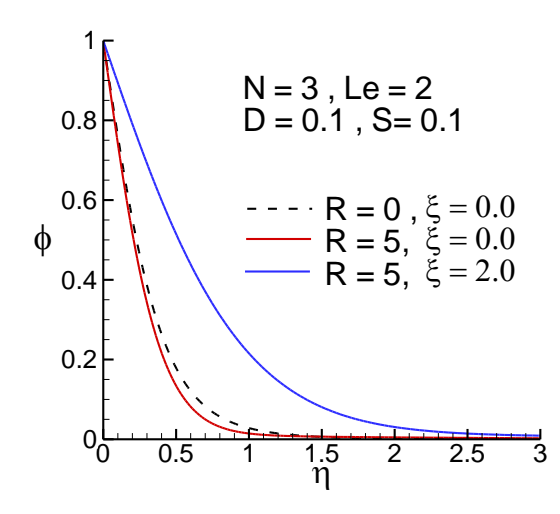


FIG. 3 The dimensionless concentration distributions for two values of ξ and R

Tables 2 and 3 display respectively the values of the Nusselt number $Nu/Ra^{1/2}$ and the Sherwood number $Sh/Ra^{\frac{1}{2}}$ for various values of the dimensionless coordinate ξ and the radiation parameter R with N = 3, Le = 2, D = 0.1, S = 0.1. First, for a fixed R, increasing the dimensionless coordinate ξ reduces monotonically both the Nusselt and Sherwood numbers. This is because increasing the dimensionless coordinate ξ increases the thermal and concentration boundary layer thicknesses, as illustrated in Figs. 2 and 3. The greater the thermal (concentration) boundary layer thickness, the smaller the Nusselt (Sherwood) number. Second, for the fixed value of ξ , increasing the radiation parameter R enhances not only the Nusselt number but also the Sherwood number. On the one hand, it is because that in the pure convection heat transfer (R=0), the Nusselt number is only proportional to the dimensionless surface temperature gradient $\left|-\theta'(\xi,0)\right|$. For the case of large R value (the thermal radiation effect is pronounced), although $[-\theta'(\xi,0)]$ is low, as shown in Fig. 2, the Nusselt number is still large. This is because the Nusselt number is found to be more sensitive to R than $[-\theta'(\xi,0)]$, as revealed in equation (29). On the other hand, when the radiation parameter R is increased, surface concentration dimensionless gradient $[-\phi'(\xi,0)]$ is also enhanced, as illustrated (black dashed line and red line) in Fig. 3. With the aid of equation (30), the larger the dimensionless surface concentration gradient, the greater the Sherwood number.

Table 2 Values of $Nu/Ra^{\frac{1}{2}}$ for various values of ξ and R with

$$N = 3$$
, $Le = 2$, $D = 0.1$, $S = 0.1$

ξ	$Nu/Ra^{\frac{V_2}{2}}$			
5	R = 0	R = 1	R=5	
0.0	1.4854	2.0104	3.1282	
0.5	1.4238	1.9271	2.9985	
1.0	1.2432	1.6826	2.6181	
1.5	0.9572	1.2955	2.0157	
2.0	0.5968	0.8077	1.2568	
2.5	0.2336	0.3162	0.4920	
3.0	0.0128	0.0173	0.0269	
π	0.0000	0.0000	0.0000	

Table 3 Values of $Sh/Ra^{\frac{1}{2}}$ for various values of ξ and R with

N = 3, Le = 2, D = 0.1, S = 0.1

ξ	$Sh/Ra^{\frac{1}{2}}$		
5	R = 0	R = 1	R = 5
0.0	2.4487	2.5686	2.6506
0.5	2.3472	2.4621	2.5408
1.0	2.0495	2.1498	2.2185
1.5	1.5780	1.6553	1.7082
2.0	0.9839	1.0321	1.0651
2.5	0.3852	0.4041	0.4170
3.0	0.0211	0.0221	0.0228
π	0.0000	0.0000	0.0000

Figures 4 and 5 show the dimensionless temperature and concentration profiles for two values of the Dufour parameter D (D = 0.0, 0.3)

and the Soret parameter S (S = 0.0, 0.3) with N= 3, Le = 2, R = 1, ξ = 0, respectively. For the case of S = 0.3, enhancing the Dufour parameter D from 0.0 to 0.3 reduces the dimensionless surface temperature gradient $[-\theta'(\xi,0)]$, but enhances the dimensionless surface concentration gradient $[-\phi'(\xi,0)]$. On the contrary, for D=0.0case, an increase in the value of the Soret parameter S from 0.0 to 0.3 tends to enhance the dimensionless surface temperature gradient $[-\theta'(\xi,0)]$, as shown in Fig. 4, but decreases the dimensionless surface concentration gradient $[-\phi'(\xi,0)]$, as illustrated in Fig. 5.

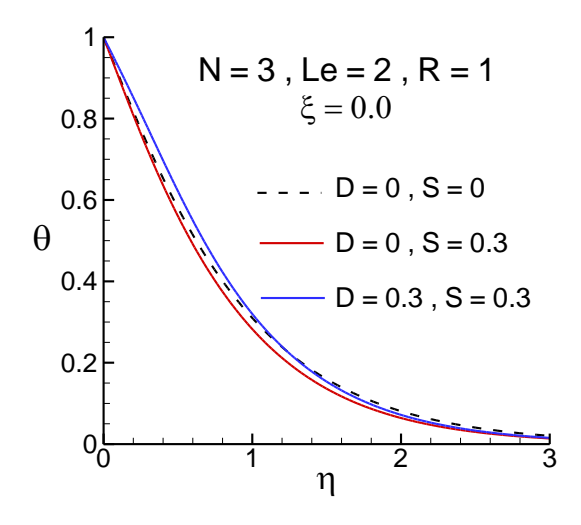


FIG. 4 The dimensionless temperature profiles for two values of D and S

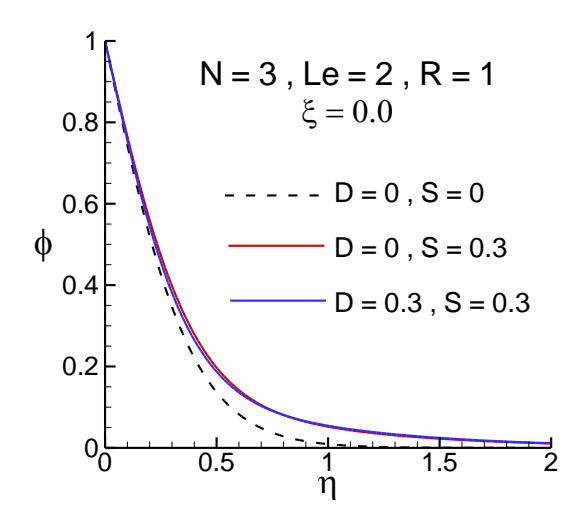


FIG. 5 The dimensionless concentration profiles for two values of D and S

The values of the Nusselt number $Nu/Ra^{\frac{1}{2}}$ and the Sherwood number $Sh/Ra^{\frac{1}{2}}$ for various values of ξ , D and S with N=3, Le=2, R=1, are shown in Tables 4 and 5, respectively. On the one hand, for the fixed S, increasing the Dufour parameter D decreases the Nusselt number but increases the Sherwood number. This is because the fact that as the Dufour parameter D is enhanced, the dimensionless surface temperature gradient $[-\theta'(\xi,0)]$ reduces but the dimensionless surface concentration gradient $[-\phi'(\xi,0)]$ enhances, as illustrated in Figs. 4 and 5, respectively. On the other hand, for the fixed value of D, increasing the Soret parameter S enhances (decreases) the Nusselt (Sherwood) number.

Table 4 Values of $Nu/Ra^{1/2}$ for various values of ξ , D and S with

$$N = 3$$
, $Le = 2$, $R = 1$

	$Nu/Ra^{\frac{1}{2}}$			
ξ	D=	0.0	D = 0.3	
	S = 0.0	S = 0.3	S = 0.0	S = 0.3
0.0	2.1704	2.2810	1.5604	1.6959
0.5	2.0804	2.1864	1.4957	1.6256
1.0	1.8164	1.9090	1.3059	1.4193
1.5	1.3985	1.4698	1.0054	1.0928
2.0	0.8720	0.9164	0.6268	0.6813
2.5	0.3414	0.3588	0.2454	0.2667
3.0	0.0187	0.0197	0.0134	0.0146
π	0.0000	0.0000	0.0000	0.0000

Table 5 Values of $Sh/Ra^{\frac{1}{2}}$ for various values of ξ , D and S with

$$N = 3$$
, $Le = 2$, $R = 1$

	$Sh/Ra^{\frac{1}{2}}$			
ξ	ξ $D=0$.		D = 0.3	
	S = 0.0	S = 0.3	S = 0.0	S = 0.3
0.0	2.6277	2.4006	2.6452	2.5081
0.5	2.5188	2.3012	2.5356	2.4041
1.0	2.1993	2.0093	2.2139	2.0992
1.5	1.6934	1.5471	1.7047	1.6163
2.0	1.0559	0.9646	1.0629	1.0078
2.5	0.4134	0.3776	0.4161	0.3946
3.0	0.0226	0.0207	0.0228	0.0216
π	0.0000	0.0000	0.0000	0.0000

4. Conclusion

In this paper, a boundary layer analysis is presented to study the effects of thermal radiation, Dufour and Soret on natural convection flow in a saturated porous medium resulting from combined heat and mass buoyancy effects adjacent to the sphere maintained at uniform wall temperature and concentration. The main governing parameters of the problem are the dimensionless coordinate ξ , the radiation parameter R, the Dufour parameter D, the Soret parameter S. The results of present study

are as follows:

- I. Increasing the dimensionless coordinate ξ reduces both the Nusselt number and the Sherwood number.
- II. Enhancing the radiation parameter R increases the Nusselt number as well as the Sherwood number.
- III. When the Dufour parameter D is increased, the Nusselt (Sherwood) number is reduced (enhanced).
- IV. As the Soret parameter S increases, the Nusselt number tends to increase yet the Sherwood number has the tendency to decrease.

References

- Bejan, A., Convection heat transfer, 4th edn. Wiley, New York (2013).
- [2] Nield D. A., and Bejan, A., Convection in porous media, 5th edn. Springer, New York (2017).
- [3] Yamamoto, K., "Natural convection about a heated sphere in a porous medium," Journal of the Physical Society Japan, Vol. 37, pp. 1164-1166 (1974).
- [4] Merkin, J. H., "Free convection boundary layers on axi-symmetric and two-dimensional bodies of arbitrary shape in a saturated porous medium," International Journal of Heat and Mass Transfer, Vol. 22, pp. 1461-1462 (1979).
- [5] Cheng, P., "Mixed convection about a horizontal and a sphere in a fluid-saturated porous medium," International Journal of Heat and Mass Transfer, Vol. 25, pp. 1245-1247 (1982).
- [6] Minkowycz, W. J., Cheng, P., and Chang, C. H., "Mixed convection about a nonisothermal

- cylinder and sphere in a porous medium," Numerical Heat Transfer, Vol. 8, pp. 349-359 (1985).
- [7] Huang, M. J., Yih, K. A., Chou, Y. L., and Chen, C. K., "Mixed convection flow over a horizontal cylinder or a sphere embedded in a saturated porous medium," ASME Journal of Heat Transfer, Vol. 108, pp. 469-471 (1986).
- [8] Nakayama, A., and Koyama, H., "Free convective heat transfer over a nonisothermal body of arbitrary shape embedded in a fluid-saturated porous medium," ASME Journal of Heat Transfer, Vol. 109, pp. 125-130 (1987).
- [9] Pop, I., and Yan, B., "Forced convection flow past a circular cylinder and a sphere in a Darcian fluid at large Peclect numbers," International Communications in Heat and Mass Transfer, Vol. 25, pp. 261-267 (1998).
- [10] Yih, K. A., "Viscous and Joule heating effects on non-Darcy MHD natural convection flow over a permeable sphere in porous media with internal heat generation," International Communications in Heat and Mass Transfer, Vol. 27, pp. 591-600 (2000).
- [11] Cheng, C. Y., "Free convection heat transfer from a sphere in a porous medium using a thermal non-equilibrium model," Transport in Porous Media, Vol. 98, pp. 209-221 (2013).
- [12] Lai, F. C., and Kulacki, F. A., "Coupled heat and mass transfer from a sphere buried in an infinite porous medium," International Journal of Heat and Mass Transfer, Vol. 33, pp. 209-215 (1990).
- [13] Chamkha, A. J., Gorla, R. S. R., and Ghodeswar, K., "Non-similar solution for convective boundary layer flow over a sphere

- embedded in a porous medium saturated with a nanofluid," Transport in Porous Media, Vol. 86, pp. 13-22 (2011).
- [14] Huang, C. J., "Influence of non-Darcy and MHD on free convection of non-Newtonian fluids over a vertical permeable plate in a porous medium with Soret/Dufour effects and thermal radiation," International Journal of Thermal Sciences, Vol. 130, pp. 256-263 (2018).
- [15] Moorthy, M. B. K., Kannan, T., and Senthilvadivu, K., "Soret and Dufour effects on natural convection heat and mass transfer flow past a horizontal surface in a porous medium with variable viscosity," WSEAS Transactions on Heat and Mass Transfer, Vol. 8, pp. 121-131 (2013).
- [16] Huang, C. J., "Soret/Dufour effects on coupled heat and mass transfer by free convection over a vertical permeable cone in porous media with internal heat generation and thermal radiation," Heat Transfer Research, Vol. 48, pp. 1203-1216 (2017).
- [17] Cheng, C. Y., "Soret and Dufour effects on free convection boundary layer over a vertical cylinder in a saturated porous medium," International Communications in Heat and Mass Transfer, Vol. 37, pp. 796-800 (2010).
- [18] Yih, K. A., "Free convection about a permeable horizontal cylinder in porous media with Soret/Dufour effects: UHF/UMF," Journal of Air Force Institute of Technology, Vol. 19, pp. 1-12 (2019).
- [19] Huang, C. J., and Yih, K. A., "Nonlinear radiation and variable viscosity effects on free convection of a power-law nanofluid over a truncated cone in porous media with zero

航空技術學院學報 第二十二卷 (民國一一二年)

nanoparticles flux and internal heat generation," Journal of Thermal Science and Engineering Applications, Vol. 13, pp. 031020-1–11 (2021).